Geophysical Prospecting

EAGE EUROPEAN ASSOCIATION OF GEOSCIENTISTS & ENGINEERS

Geophysical Prospecting, 2015 doi: 10.1111/1365-2478.12277

Seismic imaging through the volcanic rocks of the Snake River Plain: insights from Project Hotspot

Lee M. Liberty[1]*, Douglas R. Schmitt[2] and John W. Shervais[3]

[1]*Boise State University, Department of Geosciences, 1910 University Drive, Boise, ID 83725-1536, USA,* [2]*Institute for Geophysical Research, Department of Physics, University of Alberta, Edmonton, AB T6G 2E1, Canada, and* [3]*Department of Geology, Utah State University, 4505 Old Main Hill, Logan, UT 843224905, USA*

Received September 2014, revision accepted March 2015

ABSTRACT

Hotspot: The Snake River Geothermal Drilling Project was undertaken to better understand geothermal systems across the Snake River Plain volcanic province. A series of surface and borehole seismic profiles were obtained to provide insights into volcanic stratigraphy and test the capabilities of engineering-scale seismic imaging in such terranes. The Kimberly site drilled through 1.9 km of mostly rhyolite, with thin sedimentary interbeds in the upper part of the section. The Kimama site drilled through 1.9 km of mostly basalt with sedimentary interbeds at ~200 m depth and 1700 m depth. The Mountain Home site contained numerous sediment and volcanic rock layers. Downhole and surface vibroseis seismic results suggest sedimentary interbeds at depth correspond with low-velocity, high-temperature zones that relate to reflections on seismic profiles. Our results suggest that eruption flow volumes can be estimated and flow boundaries can be imaged with surface seismic methods using relatively high-fold and wide-angle coverage. High-frequency attenuation is observed at all sites, and this deficit may be countered by acquisition design and a focus on signal processing steps. Separation of surface and body waves was obtained by muting, and the potential for large static effects was identified and addressed in processing. An accurate velocity model and lithology contacts derived from borehole information improved the confidence of our seismic interpretations.

Key words: Seismic Imaging, Geothermal, Volcanic Rocks.

INTRODUCTION

Project Hotspot is an international collaborative effort to explore the heat distribution within the Snake River Plain volcanic province (Shervais *et al.* 2011), which is one of the highest heat flow regions of North America (Fig. 1). The geologic framework for this intermountain province was strongly influenced by the passing Yellowstone hotspot (e.g., Shervais and Hanan 2008) and contains a complex distribution of eruptive volcanic centres, rhyolite and basaltic flows, sedimentary layers, and fracture systems, Because the geothermal resources are located at depth with little to no surface expression, Project Hotspot has utilized geophysical, geological, and geochemical techniques to better understand the heat distribution and to identify pathways for fluid flow. Here, we discuss surface and borehole seismic data that were acquired to identify key lithologic and hydrogeologic boundaries that are relevant to geothermal exploration in this volcanic province. We focus our study on geothermal resources located in the upper 2 km. To date, seismic imaging within such complex geological environments has been limited, in part, by the large seismic velocity and density contrasts between volcanic rocks and the often thin sediment interbeds, and the large lateral variations in volcanic flow boundaries. These

*E-mail: lliberty@boisestate.edu

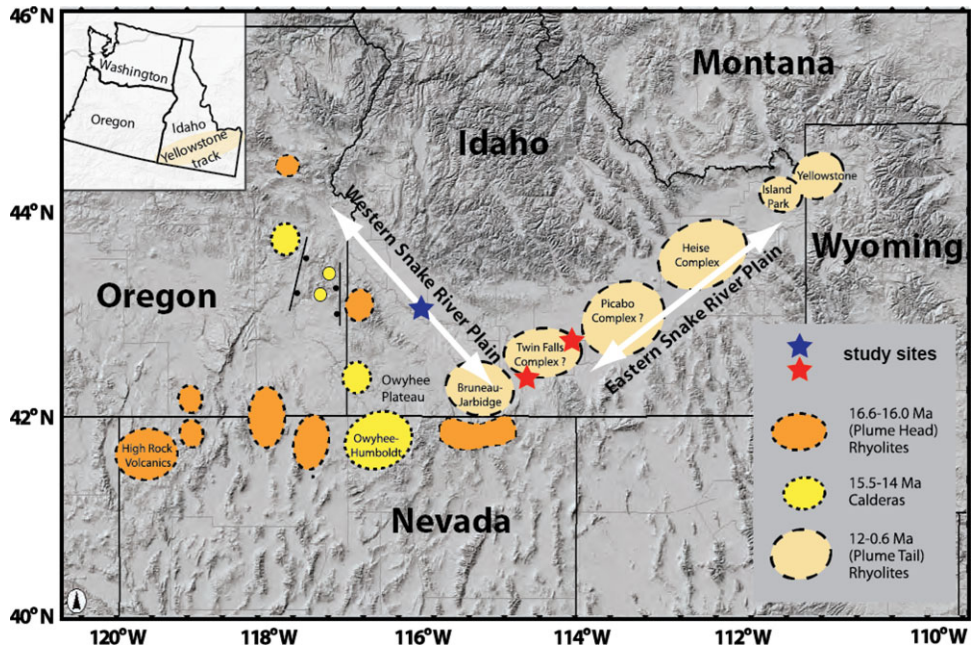

Figure 1 Digital topographic map of Southern Idaho and surrounding area of the U.S. Pacific Northwest (inset map) showing location of eruptive centres related to the track of the Yellowstone Hotspot (revised from Shervais and Hannan 2008). The Kimberly and Kimama sites (red stars) are located on the perimeter of the Twin Falls eruptive complex. The Mountain Home site (blue star) is located on the eastern margin of the western Snake River Plain graben.

complexities lead to scattering, partitioning, attenuation, and large travel-time delays of the seismic wavefield (e.g., Pujol, Fuller, and Smithson 1989; Pujol and Smithson 1991; Planke, Alvestad, and Eldholm 1999; Ziolkowski *et al.* 2003).

One objective of our project was to assess seismic imaging capabilities and limitations at a number of unique geological sites within the Snake River Plain (Fig. 1). In particular, we explore for permeable pathways using a small vibratory source to image thin kilometre-deep fractures and sedimentary interbeds along the margins of a buried caldera and blind geothermal system. One site, Kimberly, is drilled into a thick rhyolite sequence that lies beneath a basalt/sediment cover. Another site, Kimama, is located in thick, overlapping sequence of basalt flows originating from a series of vents. The final site, Mountain Home, is located in a fault-bounded sedimentary basin with both surface and buried basalt layers. Here, we discuss surface and borehole results using vertical seismic profiling (VSP) and surface seismic methods to show that major flow boundaries can be imaged in these complex geologic environments. At these sites, we acquired surface and borehole seismic data using a 2720 kg peak force IVI Minivib source and 240–360 vertical 14 Hz single-sensor geophones spaced at 4 m. Our downhole (VSP) seismic data were acquired with a Sercel Slimwave three-component borehole geophone at 2 m spacing at the Kimberly and Kimama sites and a single-component vertical geophone at the Mountain Home site. We conclude that high-fold low-frequency wide-angle surface seismic data are needed to image volcanic flow boundaries. We show that seismic imaging methods can shed light on the distribution of volcanic rocks, that we can identify major volcanic flow boundaries, and that we can characterize the geometry of permeable pathways that may be conduits for upwelling geothermal waters.

KIMBERLY SITE

The Kimberley site, located along the southwest margin of the Twin Falls volcanic complex (Fig. 1), is well known for its low-enthalpy geothermal resources. Here, the ground waters are recharged in the mountains to the south and seep deeper into the crust where the water is heated, and then upwells to form an artesian system (Street and deTar 1987). The borehole and surface seismic profiles are located along the west flank of Hansen Butte, immediately south of the Snake River (Fig. 2). The site lithology includes basalt and sediment interbeds above 0.4 km and a continuous rhyolite sequence from 0.4 km to a total drilled depth of 1.95 km (Shervais *et al.* 2011; Fig. 2). A few isolated and thin sediment zones appear

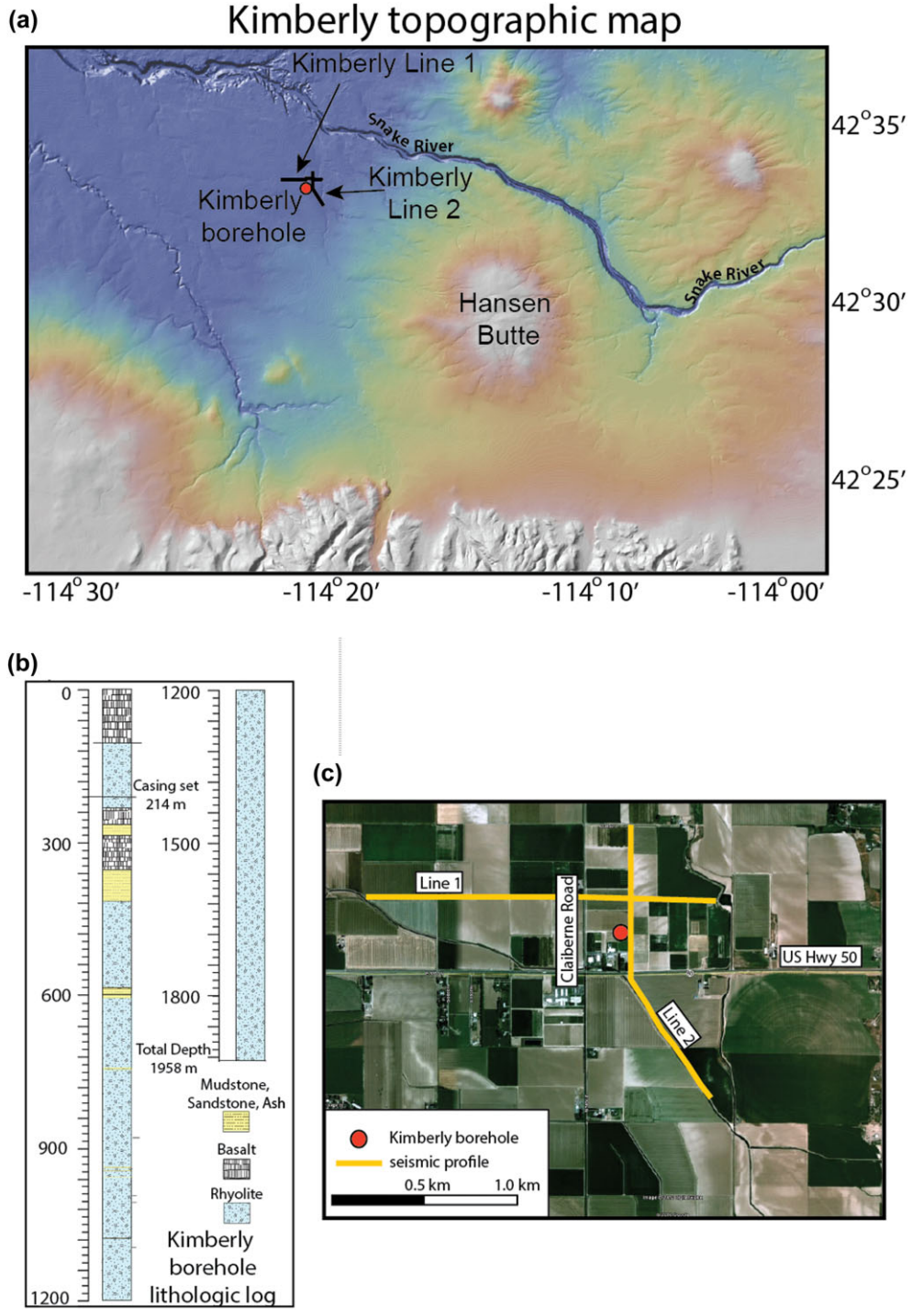

Figure 2 (a) Topographic map showing the Kimberly drill site and seismic profile locations on the northwest flank of Hansen Butte near Kimberly, Idaho. (b) Lithologic log from the Kimberly borehole. (c) Aerial photo of the Kimberly site. Seismic data were collected along farm fields.

within the rhyolite sequence, and these higher permeability volcanic boundaries are of interest as geothermal targets (e.g., Lindholm 1996; Welhan, Clemo, and Gégo 2002; Fig. 2).

Kimberly borehole seismic results

A 1.9-km-deep vertical seismic profiling (VSP) at the Kimberly site shows clear first arrivals on the vertical geophone component using a 20–160 Hz sweep P-wave vibroseis source (Fig. 3). We acquired four-fold data at a 2 m vertical station spacing, whereas the source was stationed approximately 17 m from the borehole. Using a simple bandpass filter for display (Fig. 3a), the first arrivals suggest relatively low attenuation of the P-wave seismic energy at the dominant frequency of 30–40 Hz. The less coherent arrivals on the horizontal component of the downhole data (discussed below) suggests that significant shear wave energy was not generated directly with our vibroseis source. On the vertical-component data at higher frequencies, we observe significant attenuation with increasing depth. Although we acquired data to above 100 Hz, significant direct arrival energy above this frequency was not recorded at depths greater than 0.4 km (Fig. 4). At these higher frequencies, low-velocity tube-wave arrivals (at near drilling mud velocity) and multiple downgoing arrivals that parallel the first break direct P-wave arrival dominate the VSP wave field. Although tube waves are not an issue for a surface seismic campaign, this analysis suggests that little high-frequency coherent seismic energy is returned to the surface from below the upper basalt/sediment interbeds at 0.4 km depth. However, the VSP containing a high cut filter of 60 Hz shows coherent signal to our maximum geothermal target of 2.0 km depth (Fig. 4). This high-frequency attenuation is consistent with other seismic studies conducted in volcanic regions (e.g., Pujol and Smithson 1991; Ziolkowski *et al.* 2003) and with our measurements at Kimama and Mountain Home sites. This suggests that near-surface heterogeneities can limit thin bed imaging at greater depths. With an average seismic velocity of 4500 m/s at 1 km depth (Fig. 3c), a 60 Hz signal would result in a wavelength of 75 m. Although we can resolve seismic boundaries at a fraction of a wavelength (e.g., Widess 1973), meter-scale flow boundaries at these depths likely require higher frequencies to be clearly resolved.

We picked first arrivals to estimate P-wave interval velocities (Fig. 3c). A first-order least squares fit of first-arrival times suggest a general increase from 4000 m/s near the surface to 6000 m/s at 1.9 km depth. Very large velocity variations appear within the upper basalt/sediment sequence, but the general increase in velocity with depth is typical of seismic velocity measurements with increasing confining pressure for similar igneous rocks (e.g., Christensen 1982). Low-velocity zones appear where sediment interbeds are identified in the lithologic log (Shervais *et al.* 2012), and many of these zones correlate with fluctuations in downhole water temperature (Fig. 3c; Nielson, Delahunty, and Shervais 2012). The calculated velocity values for the thin sedimentary interbeds are likely overestimated due to the influence of the high rhyolite seismic velocities that lie above and below the interbeds, and a smoothing filter used to calculate interval velocity values. However, thick sedimentary interbeds observed at depths of 0.4 km and 0.6 km record interval velocities of 2000–3000 m/s and represent fine-grained unconsolidated sediments that were logged within these zones (Shervais *et al.* 2011). In summary, we observe a general increase in seismic velocity of approximately 1000 m/s per km within the rhyolite sequence and slow seismic velocities that correlate with sedimentary interbeds at the Kimberly site. The temperature log for this well (Fig. 3c) suggests that many of these sediment interbeds contain higher temperatures than the surrounding rocks (Nielson *et al.* 2012), making these zones an exploration target for our surface seismic campaign. One exception to this seismic velocity/sediment interbed correlation is where a low-velocity zone observed at 1.65 km depth that does not correlate to a lithologic change on the core log (Shervais *et al.* 2012). Downhole temperature fluctuations at this location suggest that a key stratigraphic boundary may be present, perhaps related to a fracture zone, and this zone is of potential interest for geothermal exploration and can be mapped with seismic methods.

Removal of the downgoing VSP seismic energy using a median subtraction filter highlights (upgoing) reflections from seismic boundaries at depth (Fig. 3d). We identify reflections that intercept the VSP first arrivals at a range of geophone depths. These arrivals indicate that reflecting boundaries are present at the Kimberly site and tie to low-velocity sediment interbeds both within the VSP depth range and presumably below borehole depths. Next, we show a corridor stack (Fig. 3e) by doubling of the travel time from the filtered and stacked VSP. This display can be directly compared with a synthetic seismic response derived from the VSP interval velocity measurements, can provide a direct comparison of well depth to two-way travel time, and can be compared with our surface seismic reflection results. In particular, we correlate reflections within the outer corridor region (the zone closest to the first arrivals) to lithologic boundaries identified from core to conclude that surface seismic imaging may capture key geothermal target boundaries. These boundaries include most identified sediment interbeds and the low-velocity zone at

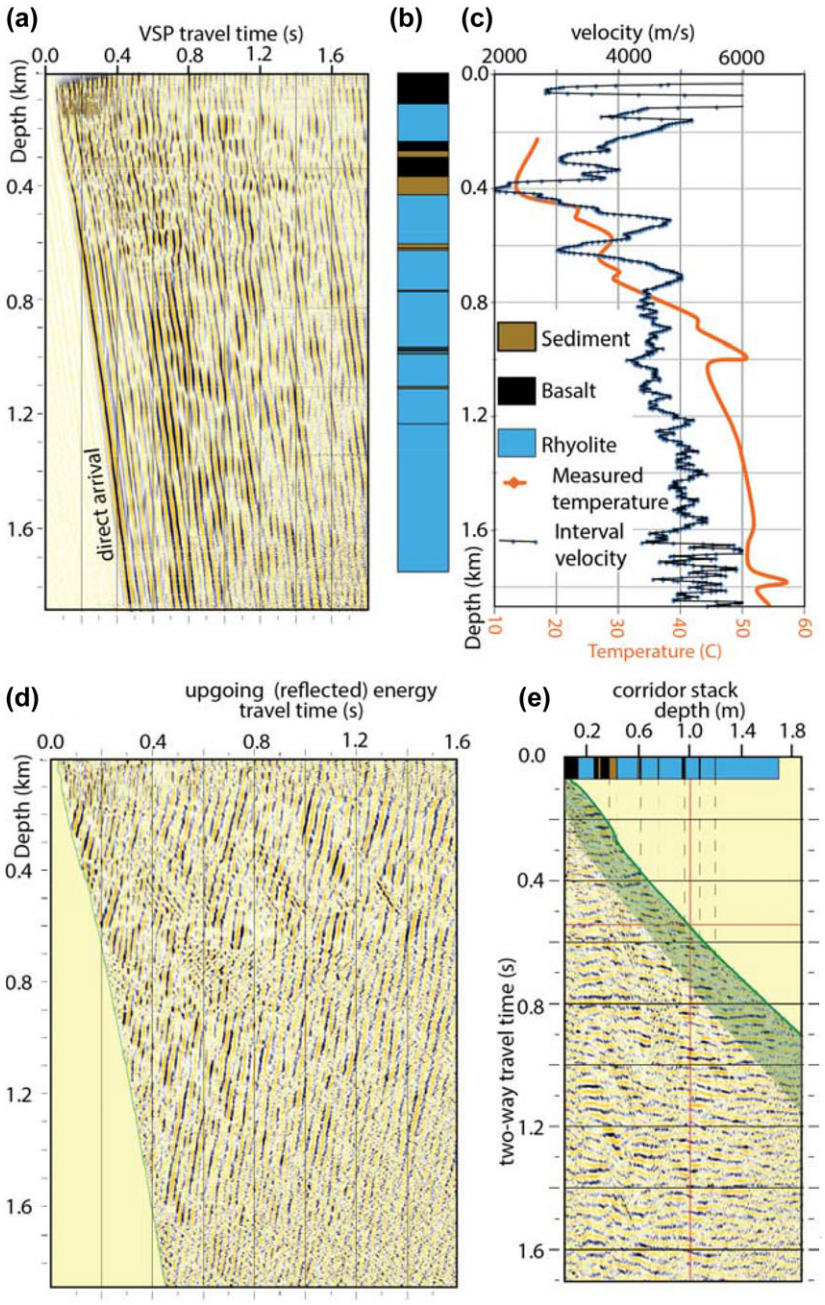

Figure 3 (a) Stacked and filtered vertical component of the Kimberly VSP to emphasize direct downgoing arrivals. (b) Generalized borehole log for the Kimberly well. (c) Interval velocity log picked from first arrivals from (a). Borehole measured temperature log shows warmer water at some sediment interbeds compared with background values (from Nielson *et al.* 2012). (d) Downgoing arrivals were removed through signal processing to emphasize reflected (upgoing) arrivals. Green line represents first-arrival travel time picks and the shaded area highlights primary reflected signals. (e) Corridor stack in two-way time used to correlate surface seismic travel time to depth. The highlighted zone represents the outside corridor region that minimizes reflection artifacts such as multiples. We highlight key lithologic boundaries (dashed lines) from the borehole log to emphasize primary reflections.

1.6 km depth. This outer corridor region emphasizes primary reflection energy and can be compared with the inner corridor area that may contain both primary, multiple, and mode-converted reflection energy (e.g., Burton and Lines 1997).

Beyond the outside region of the corridor stack, primary reflected arrivals should appear flat, lying, or return at the same travel time from all receiver depths on our corridor stack (Fig. 3e). If these reflected arrival times vary with receiver depth, these travel-time delays may imply a more complex velocity distribution than the direct first arrivals suggest. Static time shifts occur when large seismic velocities are encountered and particularly where a 1D velocity model does not accurately represent subsurface geologic conditions. To examine static or travel-time effects with surface seismic methods, we acquired a three-component walkaway VSP (Fig. 5). These data were collected by moving the vibroseis truck at

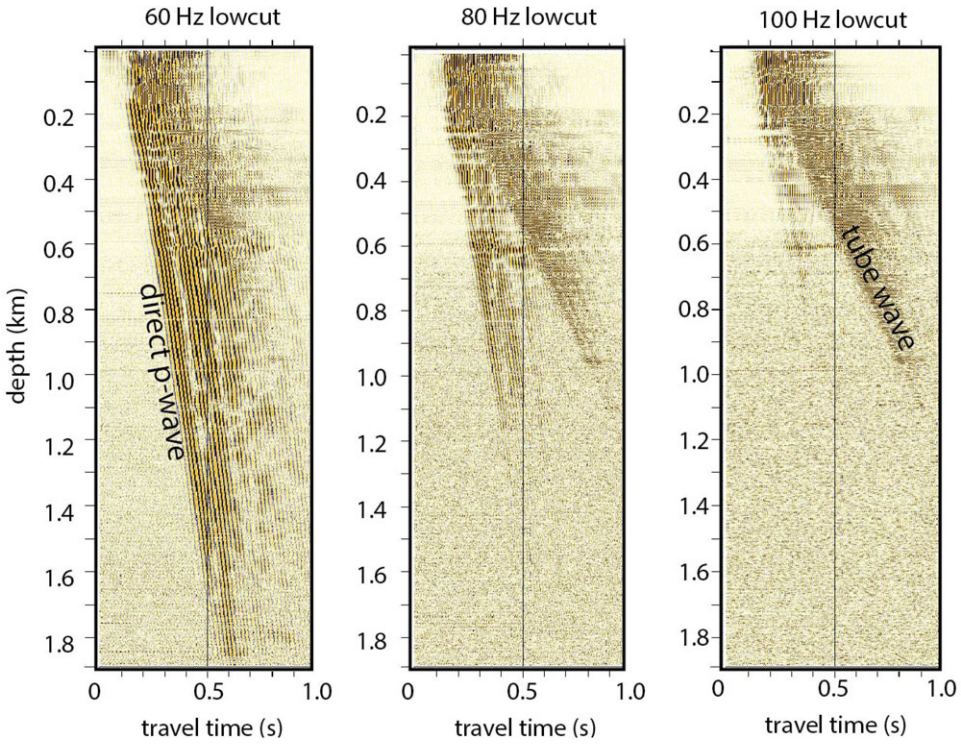

Figure 4 Filter panels from the vertical component of the Kimberly VSP showing attenuation of high-frequency signals with increasing depth. Note that little first-arrival signal above 100 Hz appears below 300 m depth.

4 m intervals along the road adjacent to the Kimberly borehole for a length of 0.42 km and for a range of receiver depths. The Kimberly borehole was located at surface position of 0.31 km. Our first-arrival picks on the vertical component of Fig. 5(a) show a large and repeatable pattern of travel-time shifts that is consistent with large lateral velocity changes within the upper few hundred metres of depth. When removing the geometrical moveout for each source/receiver pair using the velocity model shown in Fig. 3(c), static measurements of more than 60 ms (two-way travel time) appear within lateral distances of less than 50 m, and these travel-time variations are nearly identical for all depths below 0.5 km (Fig. 5b). Our analysis suggests that the majority of static effects occur in the upper few hundred metres and are likely related to lateral changes in shallow volcanic flow boundaries. At the location of the borehole, we observe two-way travel-time static shifts of nearly 30 ms, consistent with the observed fluctuations in corridor stack reflection travel times. For a centre frequency of 30 Hz, these static shifts equate to more than one wavelength and suggest that a residual static approach to surface seismic imaging may not be adequate to address these long wavelength effects.

To succeed with surface seismic imaging techniques to image deeper stratigraphy, these static effects must be addressed. Typically, these long-wavelength statics effects can be addressed with a refraction static analysis via turning ray tomography methods (e.g., Cox 1999; Schijns *et al.* 2009). However, in a province where velocity inversions from shallow volcanic layers are common, the assumptions of first-arrival tomography to extract a near-surface velocity distribution are violated. Under these conditions, borehole measurements with a layer stripping or pre-stack migration approach to reflection processing may provide the best imaging results (e.g., Martini and Bean 2002). Therefore, understanding the near-surface velocity distribution is essential to accurately image deeper strata. Borehole controls to obtain accurate seismic velocity information is therefore a critical component to high-quality surface seismic measurements. Walkaway VSP information may also provide a useful resource to understanding lateral changes in near-surface velocities.

In addition to the vertical-component data shown in Fig. 5(a), we also show the horizontal component VSP results from the walkaway test. Our results show that the relative amplitude on the horizontal components is similar to vertical-component amplitudes at many depths. Although some horizontal P-wave energy is expected in a VSP experiment due

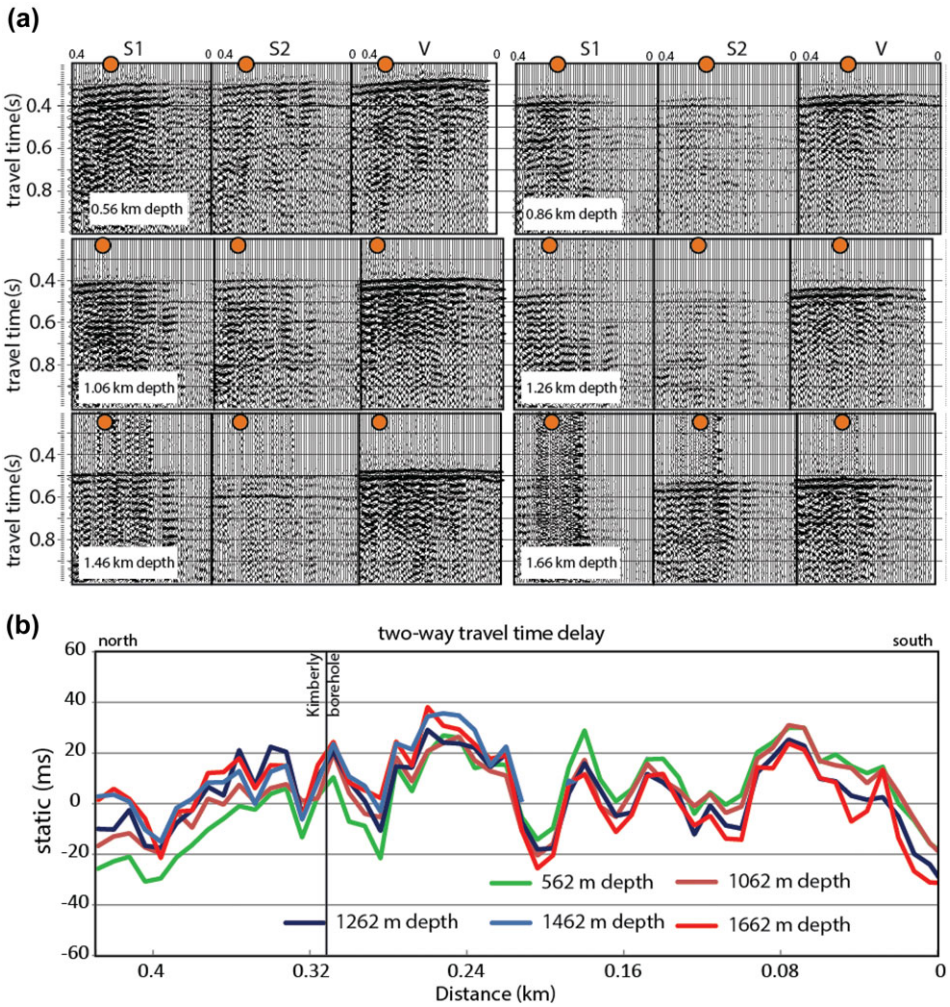

Figure 5 (a) Relative amplitude walkaway seismic profiles recorded at a range of geophone depths for horizontal (S1 and S2) and vertical (V) receivers. Orange circle represents the surface location of the Kimberly borehole. (b) Static effects from the vertical component of the walkaway survey showing two-way travel time delay times from a range of receiver depths. These data were calculated by subtracting the average direct wave velocity calculated at each receiver depth. Surface source locations were along Profile 2, and the borehole is located at position 0.31.

to non-vertical ray paths from velocity inversions and other geometrical considerations, we would expect identical travel-time arrivals for all components if we only recorded P-wave energy. Given an average V_p/V_s ratio for similar rocks (e.g., Christensen 1982), we would expect to see primary S-wave first arrivals at about 1.7 times the P-wave first-arrival time. Because we do not see a consistent arrival near this travel time, we conclude that primary S-wave energy was not generated with our seismic source. However, coherent horizontal-component signals that appear after the P-wave first arrivals and not on the vertical-component data suggest that mode-converted shear-wave energy is present. This observation is consistent with additional reflections that appear within the inner window of the corridor stack (compared with the outer corridor region) and suggests that a multi-component approach to seismic imaging may be beneficial to improving volcanic flow boundaries or identifying fractures (e.g., Hannsen *et al.* 2003; Stewart *et al.* 2003; Behara 2006). Utilizing shear-wave signals may help to better resolve thin sedimentary interbeds similar to what appears beneath the Snake River Plain. However, since we acquired only vertical-component data in profile, these converted waves are not further discussed with our surface seismic results.

Kimberly surface seismic results

Vertical-component surface seismic profiles from Kimberly were acquired along a road shoulder adjacent to the Kimberly

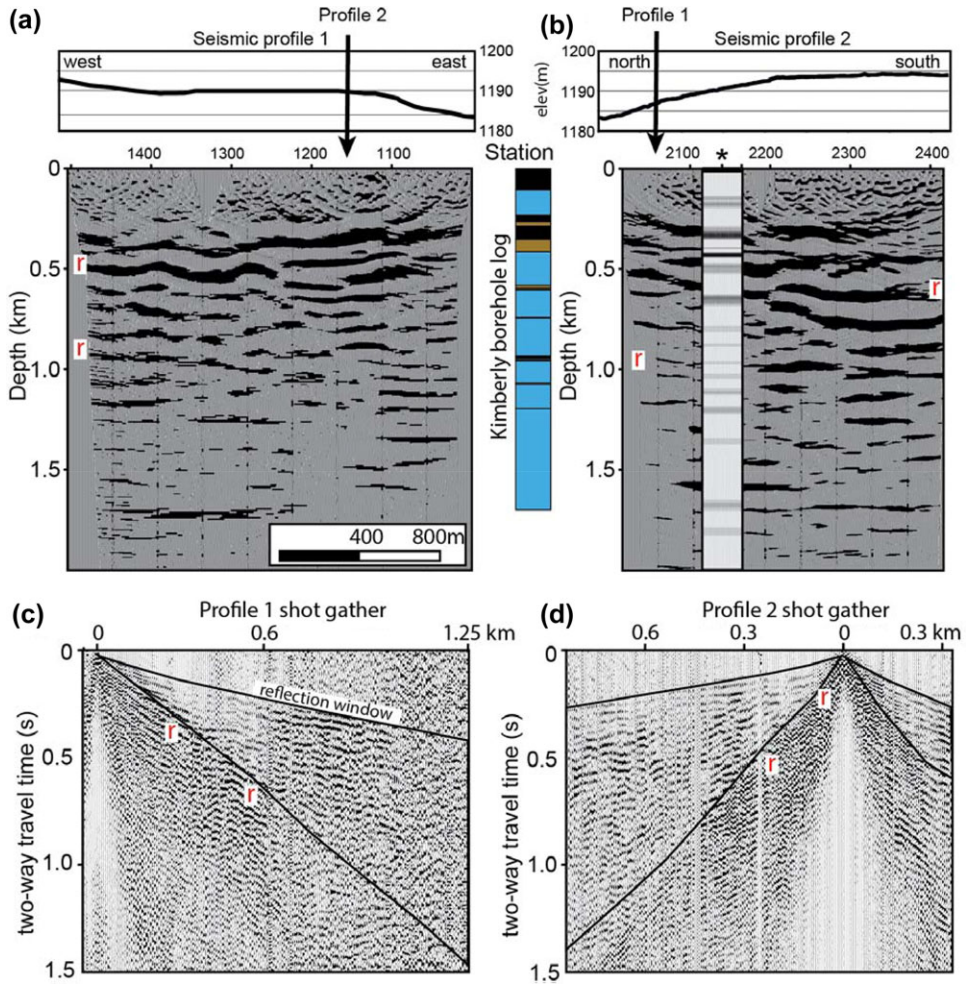

Figure 6 (a) West–East Profile 1. (b) North–South Profile 2. Migrated and depth converted surface seismic profiles from the Kimberly site with surface elevation profiles. Synthetic seismogram computed from VSP velocity profile is superimposed at the Kimberly well location on Profile 2. Note the volcanic and sedimentary rock interbeds between depths of 0.3 km and 0.6 km are imaged with surface seismic methods on both profiles. (c) Shot gather from Profile 1. (d) Shot gather from Profile 2. We identify reflections (r) on the shots that correlate with the stacked image. Stacking velocities for these reflections are consistent with VSP results.

borehole (Fig. 2). The maximum source–receiver offset with our 360-channel survey ranged from 0.72 km to 1.44 km, providing relative wide-angle coverage for the target depths upwards of 2 km. The west-to-east Profile 1 was acquired along a farm field access road, approximately 0.3 km north of the Kimberly borehole (Fig. 2). This 2-km long profile crosses seismic Profile 2 at position 1150 and Claiberne Road at position 1320. The 1.7-km-long north-to-south Profile 2 was acquired along the Kimberly well access gravel road. The profile crosses a highway at position 2200 and crosses the borehole location at position 2150. We processed these data using a standard processing approach that included pre-correlation gains to recover high-frequency signals, deconvolution, detailed velocity analyses, a focus on residual and horizon statics, and post-stack Kirchoff migration. We muted surface waves and stacked only wide-angle reflections to produce the Fig. 6 stacks. The data were depth converted using velocities derived from the VSP survey (Fig. 3).

Interbedded basalt, rhyolite, and sedimentary interbeds in the upper 1 km below the land surface provide large seismic impedance contrasts to produce a highly reflective zone observed on both Profiles 1 and 2 (Fig. 6). Profile 1 shows a near-continuous reflector that varies between depths of 0.3 km and 0.6 km and is likely associated with the sequence of near flat-lying interbedded basalt, rhyolite, and sediments observed in core and from the VSP (Fig. 3).

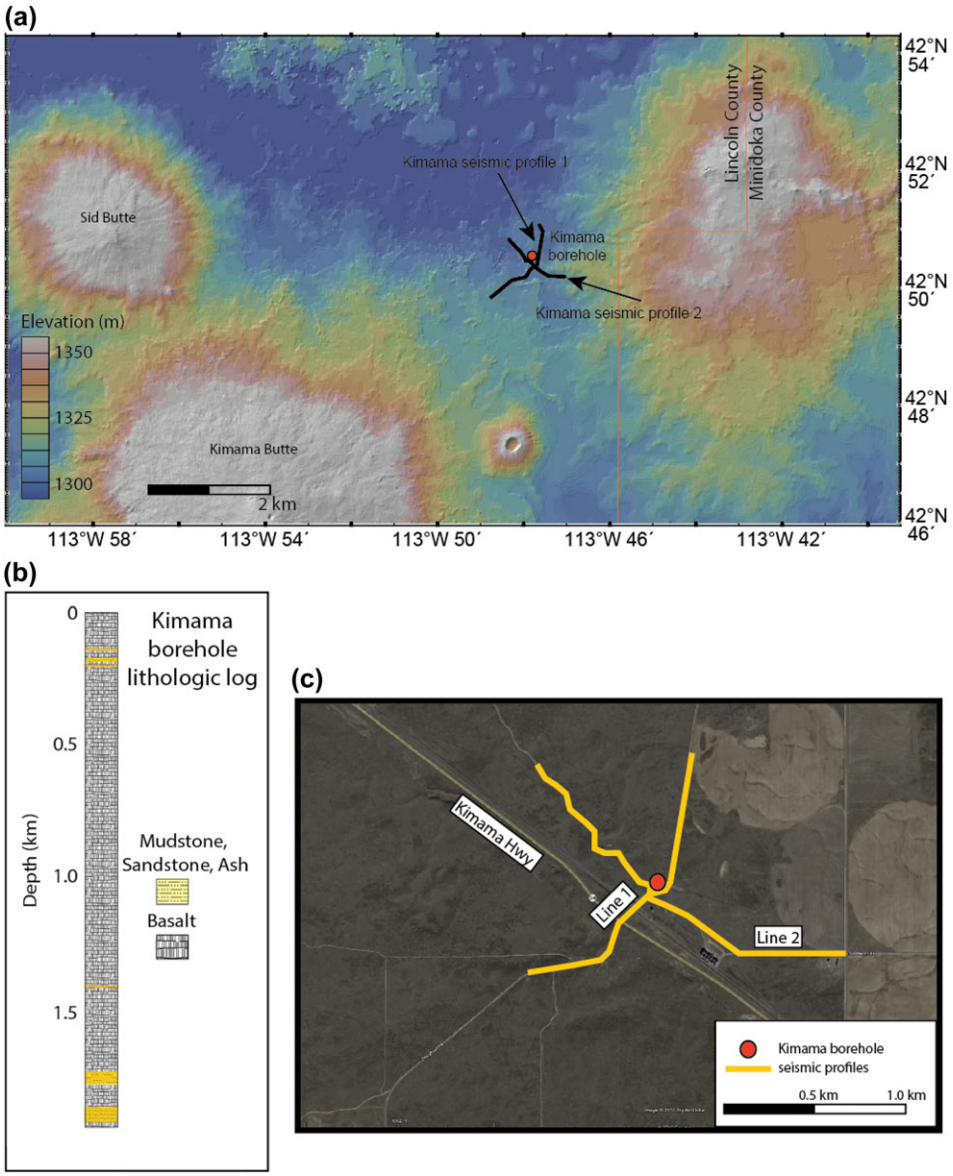

Figure 7 (a) Topographic map from the Kimama site showing borehole and surface seismic locations near multiple volcanic vents that flank the east side of the Twin Falls volcanic complex (Figure 1). (b) Generalized lithologic log from the Kimama borehole. (c) Aerial photo from the Kimama site with seismic profile and borehole locations.

These reflections are observed on most individual shot gathers (Fig. 6) and correlate with reflections from the VSP corridor stack (Fig. 3e). Deeper and more discontinuous reflectors may be associated with sedimentary interbeds observed in the borehole cores and geophysical logs (Fig. 3). A better image of these deeper interbeds may have benefited from advanced processing steps. However, poor seismic velocity estimates for the deeper reflections, in part due to a limited reflection aperture (beyond the surface-wave window) precluded a pre-stack migration approach. Although these interbeds measure less than 20 m in the Kimberly core log, lower velocity flow tops and bottoms may broaden the low-velocity zone to produce coherent arrivals at frequencies well below one seismic wavelength. These interbeds may also change thickness away from the Kimberly borehole to produce the variable reflection quality.

Profile 2 shows a package of south-dipping reflectors associated with the top of volcanic rock/sediment flow

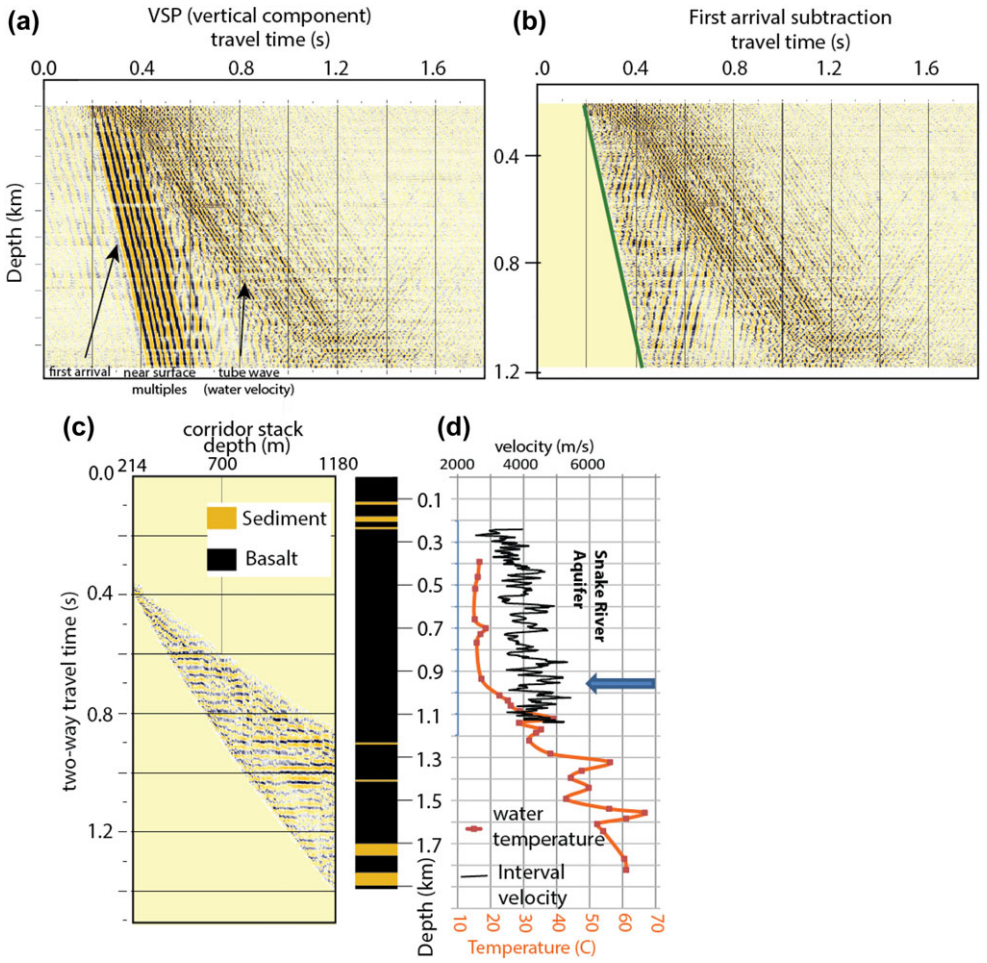

Figure 8 (a) Vertical-component VSP results from Kimama borehole. (b) Downgoing arrivals were removed through signal processing to emphasize (upgoing) reflected arrivals. Green line represents first-arrival picks. (c) Outer corridor stack in two-way travel time is used to tie VSP results to surface seismic results. Generalized borehole lithologic log showing the correlation between reflections and sediment interbeds. The tube waves were removed from this plot and the lithologic log plot was scaled to match the corridor stack from (c). (d) Interval velocity log (black line) derived from first-arrival VSP picks. Downhole temperature log (from Nielson *et al.* 2012) is also shown that tie thermal variations with seismic reflectors. The blue arrow represents the base of the Snake River cold water aquifer.

boundaries. This reflector topography on the shallower layers may suggest that the last eruptive flow associated with Hansen Butte was deposited on pre-existing topography that shallows to the north. Reflections below 0.5 km depth are more discontinuous and likely result from sedimentary interbeds observed in the borehole logs (Fig. 3), and we observe a more transparent zone of reflectivity below 1 km depth. This deeper zone is consistent with a few flow boundaries noted in the Kimberly borehole (Shervais *et al.* 2012). Large static shifts were accommodated with a residual static approach and iterative velocity analyses. This approach did not optimally address the long-wavelength static corrections (Fig. 5) but significantly improved the stack.

At the location of the Kimberly borehole on Profile 2 (Fig. 6), we inserted an acoustic synthetic seismogram derived from VSP first-arrival picks. This synthetic seismogram was derived using a 30 Hz zero-phase Ricker wavelet, similar to the observed centre-frequency recorded signals. We observe a strong correlation between reflections observed on the surface profiles and borehole seismic measurements and suggest that surface seismic imaging techniques successfully identified relatively thin volcanic flow boundaries. Because these flow boundaries and related sediment interbeds are related to fluid flow pathways and increased temperatures compared with the rhyolite sequences, we believe our surface seismic data identified geothermal targets at the Kimberly site.

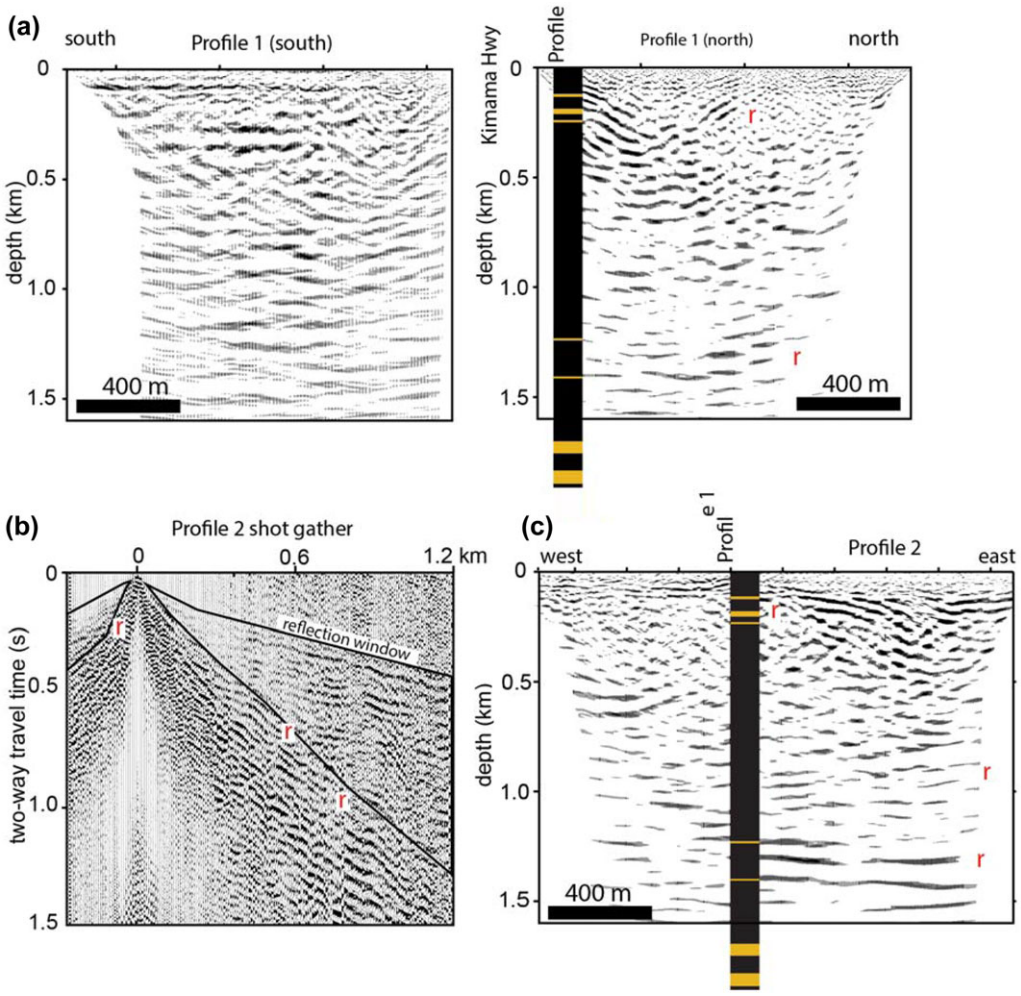

Figure 9 (a) Kimama south to north seismic Profile 1 with simplified well log at borehole location. (b) Shot gather (in time) from immediately east of the Kimama borehole. Note the reflections (r) that appear between surface wave and first-arrival windows (triangular regions) that correlate with interpreted reflections on the stacked profiles. (c) West-to-east seismic profile 2. Simplified lithology for the Kimama borehole shows basalt (black) and sediment interbeds (yellow). Profile locations are shown in Fig. 7.

KIMAMA SITE

The Kimama site is located on the eastern Snake River Plain along the eastern limits of the Twin Falls volcanic complex (Fig. 1). The surrounding region contains thick overlapping basalts that originated from a series of nearby vents (Fig. 7). The Kimama site was chosen for our studies because it sits on an axial volcanic zone that is defined by high topography to the east and by a buried basalt ridge underlying the topographic high (Lindholm 1996). The Snake River Plain cold water aquifer (Hubbell *et al.* 1997) underlies the site (Fig. 8). The aquifer is in part recharged by flow of water from the mountains to the north with the general underground flow to the southeast with significant discharge into the Snake River. The flow of these fluids cools the aquifer zone, resulting in the conductive heat transport zone not appearing until depths of about 1 km. Below the base of the Snake River aquifer at approximately 1 km depth, a higher geothermal gradient represents the geothermal exploration target of interest. The general lithology at Kimama consists primarily of basalt flows, interbedded with wind-blown sediments deposited during volcanic hiatuses in the upper 200 m and fluvial sediments at about 1700 m depth (Fig. 8; Shervais *et al.* 2012).

Kimama borehole seismic results

The Kimama vertical seismic profile (VSP) was acquired between depths of 0.2 km and 1.2 km with the same acquisition parameters described for the Kimberly survey. The data were

collected with the source stationed approximately 20 m from the borehole. Access with the VSP tool to depths less than 0.2 km and greater than 1.2 km were not possible due to the borehole conditions at the time of our seismic survey.

The vertical component from our borehole seismic results shows strong P-wave first arrivals with a seismic response similar to the Kimberly survey (Fig. 8). On the vertical geophone component, a first motion arrival time of 0.37 s at 1 km depth suggests an average P-wave velocity of 2700 m/s. Interval velocity measurements derived from first-arrival picks between depths of 0.2 km and 1.0 km suggest that seismic velocities increase from ~3000 m/s to ~5000 m/s with an average interval velocity in this depth range of 4150 m/s. This velocity increase equates to an average seismic velocity gradient of 2500 m/s per km in the upper 1 km, resulting from a combination of seismic velocity with increasing confining pressure (e.g., Christensen 1982) and the presence of unconsolidated, unsaturated sediments and fractured basalts independently logged to a water table depth of 80 m (Twining and Bartholomay 2011). Although we did not survey within the vadose zone, dry unconsolidated sediments can have P-wave seismic velocities of less than 500 m/s, whereas dry basalts and other igneous rocks have measured velocities of 10%–50% below saturated rocks of the same composition (e.g., Christensen *et al.* 1973; Christensen 1982).

The coherent arrivals that parallel the first arrival on the VSP image are likely from seismic energy trapped between the low-velocity unsaturated near-surface layer and underlying higher velocity, more competent, and saturated basalt layers below (Fig. 8a). A strong series of slower velocity downgoing arrivals matches water velocity speeds (~1500 m/s) and is consistent with tube-wave energy coupled to the borehole.

Removal of the downgoing first-arrival seismic energy using a median subtraction filter highlights the upgoing reflections to depths that approach 2 km depth (Fig. 8b). Many of the prominent reflections that we identify from the corridor stack (Fig. 8c) lie below the VSP sampling depth but within the depth where core was recovered. These reflections within the outside corridor region correlate with flow boundaries and sediment interbeds that are logged in the Kimama well (Shervais *et al.* 2012). One reflector at 0.7 km depth correlates with a warm temperature zone, but this reflector does not correlate with a major volcanic flow boundary or sediment interbed, and we do not identify this reflector from our surface seismic results. A zone between depths of 1.1 and 1.6 km (with two-way travel time from 0.9 s to 1.2 s) contains numerous reflections and is consistent with the transition from relatively uniform Snake River Aquifer volcanic rocks to a zone that includes numerous sedimentary interbeds with higher water temperatures (Fig. 8e; Nielson *et al.* 2012). Our VSP results at Kimama again suggest that sedimentary interbeds and volcanic flow boundaries at geothermal target depths within volcanic terranes can be seismically mapped. However, we observed no clear change in seismic velocity at the base of the cold water aquifer (Fig. 8e), suggesting that this boundary does not consist of a measureable change in seismic velocity or rock density.

Kimama surface seismic results

We acquired three 360-channel surface vibroseis profiles along gravel roads near the Kimama borehole (Fig. 7). We acquired two 1.4-km-long south-to-north profiles that we term Profile 1. The two profile segments are separated by a rural highway. The Kimama borehole is located immediately north of the highway along the southern limit of the northern profile segment (Fig. 9). The 2.0-km west-to-east Profile 2 crosses to within a few metres of the Kimama borehole. The western portion of this profile was acquired on an unimproved dirt road, whereas the eastern portion of the profile was shot on a regularly travelled gravel road. We processed each profile by in a similar manner to the Kimberly profiles.

Surface seismic results show reflections associated with shallow (< 0.2 km) sedimentary/basalt interbeds (Fig. 9) that were logged in the Kimama borehole but were not imaged in the VSP due to our survey restrictions (Fig. 8). These reflections that mostly appear between the surface wave and first-arrival window (Fig. 9b) suggest considerable flow topography in the upper few hundred metres depth away from the Kimama borehole that may reflect changing eruptive sources from different nearby volcanic vents (Fig. 7). These reflections from volcanic flow boundaries suggest that the younger (shallower) flows were deposited on pre-existing topography or the result of surface erosion. More coherent reflections to the north of Kimama borehole within the upper 0.5 km when compared with the profile to the south may be related to a straighter road geometry (and thus higher fold) compared with the winding road to the south (Fig. 7). Profile 2 (Fig. 9) shows reflections that match shallow sedimentary interbeds, with increasing reflector topography towards the east. The far eastern portion of this profile suggests an additional volcanic unit may sit upon the flows logged in the Kimama borehole. Deeper reflections are best observed on the west–east profile where coherent reflections are observed between depths of 1.1 km and 1.5 km or two-way travel time of 0.8 s and 1.1 s. These reflections in both VSP (Fig. 8) and the surface

seismic results (Fig. 9) show a surprising coherency that represent this sedimentary interbeds observed in the borehole logs. Poor data quality below 1.5 km depth likely represents a decrease in signal returns, perhaps from more complex wave-field conditions, and a narrow aperture with respect to imaging depths and optimum reflection window beyond the surface-wave window. To provide an improved image of the deeper targets, longer profiles would provide this greater ray path aperture by recording longer source–receiver offsets. Profile orientation in this complex geologic environment may also be a factor (Fig. 9). For example, acquiring a seismic profile along an orientation that minimizes flow boundary topography between may help reduce the effects of scattering.

MOUNTAIN HOME SITE

The Mountain Home site (Fig. 1), located on and adjacent to the Mountain Home Air Force Base, Idaho, is a site with the planned installation of a binary power system (Fig. 10). The primary goal of the Mountain Home drill core was to assess the regional geothermal potential, building on results from earlier geothermal test wells (e.g., Arney *et al.* 1982). A bottom-hole temperature of 192°C was encountered at a nearby well at a depth of 2.9 km, and similar temperatures and geothermal gradient were anticipated at the Mountain Home site. Geologically, the Mountain Home borehole sits upon surface Quaternary basalt flows that range in thickness to more than 0.2 km (e.g., Jenks, Bonnichsen, and Godchaux 1998). Below, near-shore sediments that occupy the western Snake River Plain are found to depths that exceed 0.6 km (e.g., Wood 1994; Figs. 1 and 11). Below 0.7 km depth, Tertiary basalts and sediment interbeds are encountered to the bottom of the borehole at 1.83 km depth.

Mountain Home borehole seismic results

A 1.2-km-deep vertical seismic profile (VSP) at the Mountain Home site shows clear first arrivals using a vibroseis source stationed approximately 15 m from the Mountain Home borehole (Fig. 11). The first arrivals in the upper 0.3 km show a high-velocity arrival related to the steel casing that masks the underlying (and slower) direct arrival through the formation. As with the Kimberly and Kimama wells, we observe relatively low attenuation of the P-wave seismic energy at the dominant frequency of 30 Hz–40 Hz, but at higher frequencies, we observe similar attenuation as shown in Fig. 4.

We picked first arrivals to estimate P-wave interval velocities (Fig. 11). A first-order least squares fit to the calculated interval velocities suggests a general increase from 3000 m/s near the bottom of casing to ~5000 m/s at 1.0 km depth. The direct velocity measurement at the bottom of casing suggests the upper 0.3 km contains an average velocity of 2800 m/s. This velocity is consistent with near-surface basalt layers that appear in nearby boreholes and are mapped on the surface (e.g., Jenks *et al.* 1998). The sediment-dominated zone between 0.4 and 0.7 km depths are paleo-lake Idaho strata (Wood 1994). Due to the required smoothing filter, the seismic velocities for the thin volcanic rock interbeds within this zone are likely undervalued. Below 0.9 km depth, we observe higher seismic velocities, consistent with a zone that contains more basalt than the overlying lithogies.

Removal of the downgoing VSP seismic energy shows many reflections that tie to sediment interbeds both at and below VSP depths. Our corridor stack (Fig. 11c) shows two key seismic boundaries at depth of 0.75 km and 0.89 km represent the top of volcanic layers and suggest these Tertiary basalts can be imaged with surface seismic techniques. A temperature log recorded moderate temperatures in the upper 1 km depth (Nielson *et al.* 2012; Fig. 11) and confirmed that higher temperatures needed for power generation require drill-hole depths greater than 1.2 km. We acquired our surface and borehole seismic data primarily as an imaging assessment for characterizing volcanic stratigraphy in the upper 1 km at this site.

Surface seismic results

Seismic reflection results show high-amplitude arrivals and diffractions at near-surface depths, consistent with near-surface interbedded basalt and sediment layers (Fig. 12). Below the shallowest layers of Quaternary basalts (Qb), we identify a relatively transparent reflection zone. At depths from 0.6 km to more than 1 km, we identify a reflector that matches the depth of the Tertiary basalt (Tb) top, where a nearby deep borehole logs basalt and sediment interbeds to more than 3 km depth (Arney *et al.* 1982). This reflection is more clearly imaged south of the Snake River. A large step in the Tb surface appears immediately south of the Snake River that we identify as a down-to-the-north normal fault. This interpretation is consistent with surficial geologic maps (Jenks *et al.* 1998). Poor data quality north of the river precludes a detailed interpretation of the Tb surface topography.

We observe a higher reflection coherency south of the Snake River when compared with the shot gathers acquired to the north of the river, as observed on shot gathers shown in Fig. 12. We attribute this change in data quality to a more

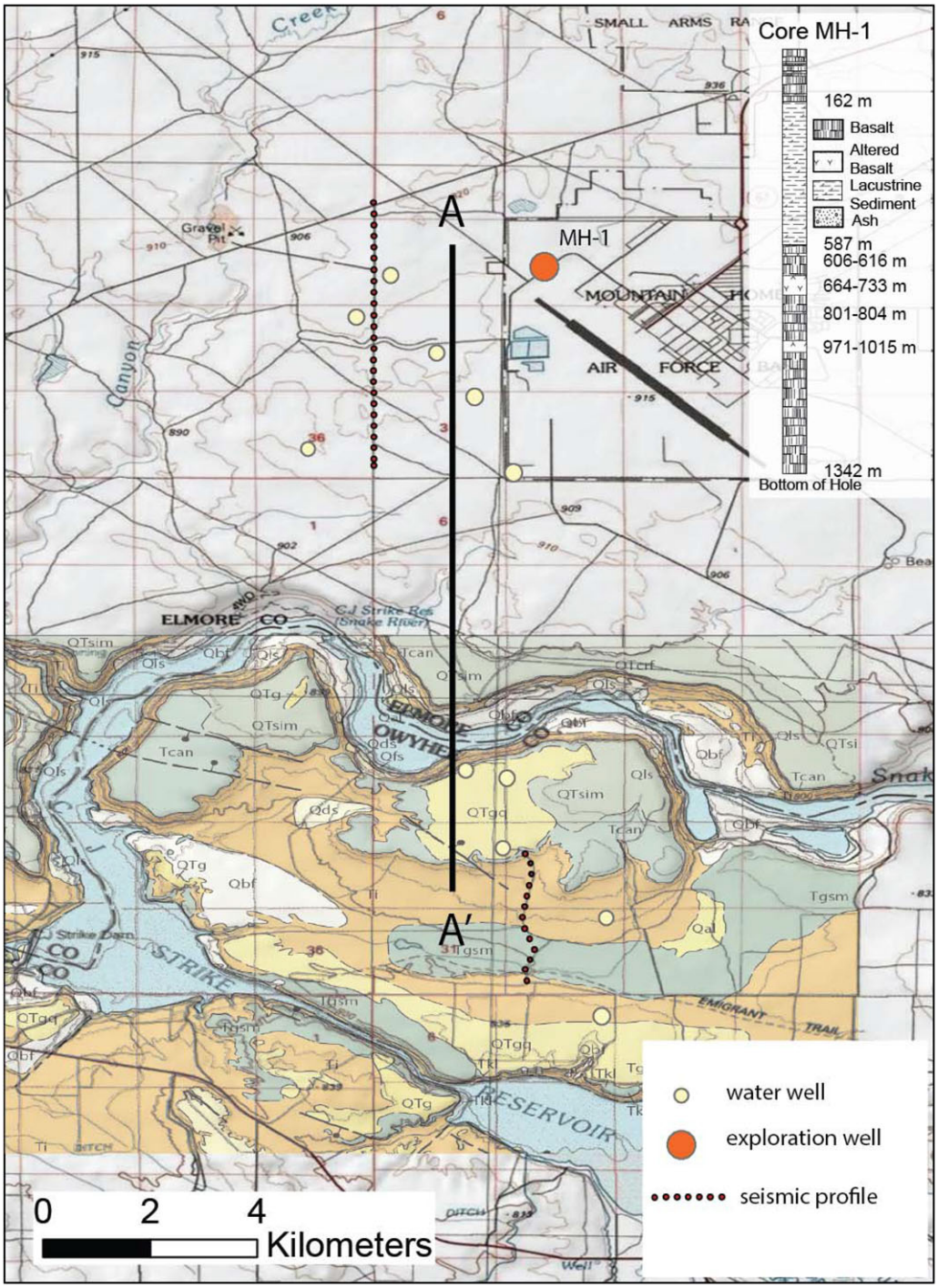

Figure 10 Topographic map for the Mountain Home area showing seismic profile locations (dots), location for Profile A-A′ (Figure 12), and generalized geological map for the region south of the Snake River (from Jenks *et al.* 1998).

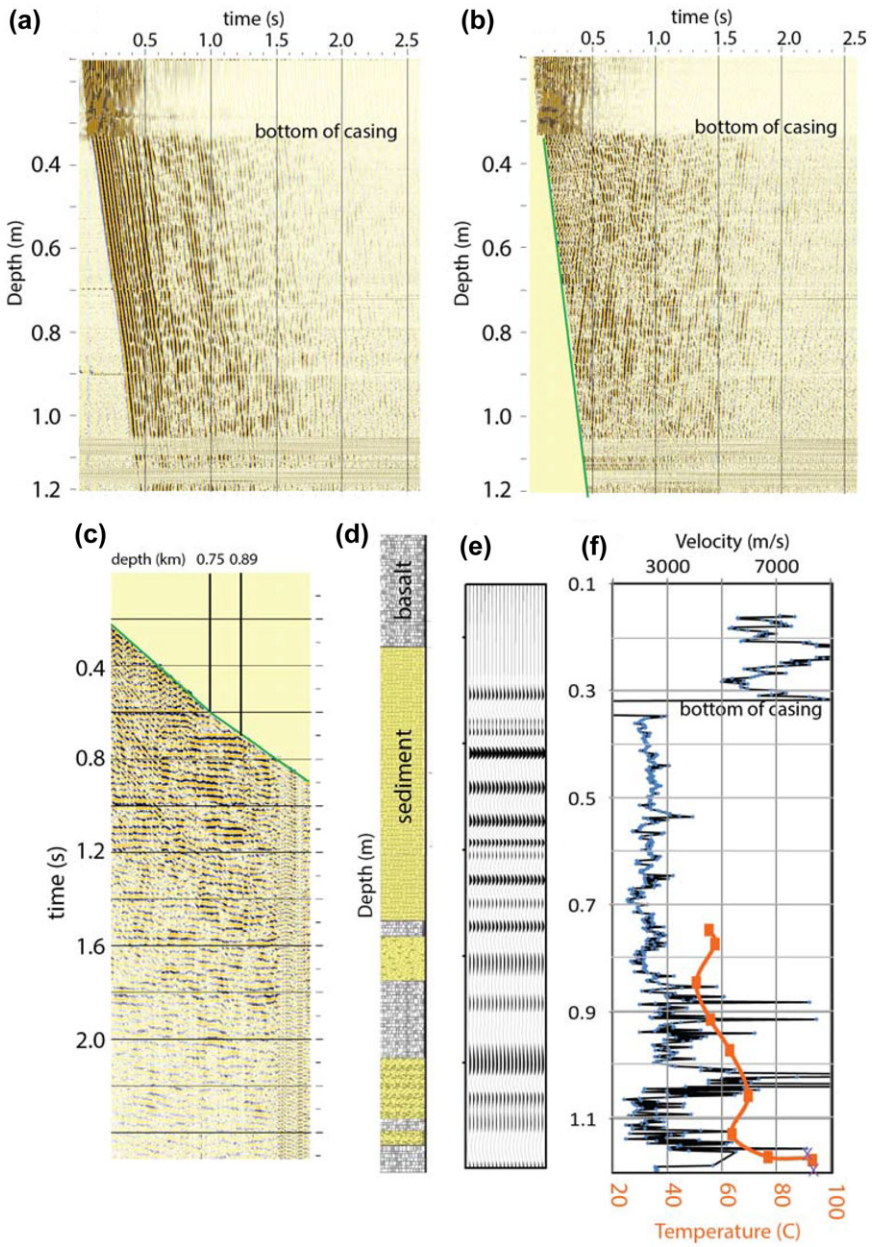

Figure 11 (a) Vertical-component VSP from Mountain Home to emphasize direct downgoing arrivals. (b) Downgoing arrival removal to emphasize reflected (upgoing) arrivals. Note that casing extends to 310 m depth and interferes with first arrival. Green line indicates first-arrival picks. (c) Corridor stack in two-way travel time is used to tie VSP results to surface seismic results. (d) Generalized borehole log from Mountain Home well. (e) Synthetic seismogram derived from interval velocities measured on (a) (f) Interval velocity log derived from first-arrival picks showing low velocities associated with lake sediments and higher velocities associated with basalt layers. Temperature log (orange line) below 700 m depth (from Nielson *et al.* 2012).

complex near-surface volcanic rock distribution and greater water table depths to the north of the Snake River compared with the area to the south. Both profile segments were acquired on hard packed gravel roads. Whereas we acquired seismic data on dry desert roads with water table depths logged to greater than 100 m to the north of the river, saturated farm fields located south of the Snake River provided an ideal coupling environment for both source and receiver. This result emphasizes that saturated materials that contain seismic velocities more similar to the shallow volcanic rock sequence reduce scattering and energy trapped in near-surface layers.

DISCUSSION

Although significant energy loss is observed from frequency attenuation, scattering, and mode conversions, we were able to image some flow boundaries related to volcanic processes at all three sites from surface and borehole seismic methods.

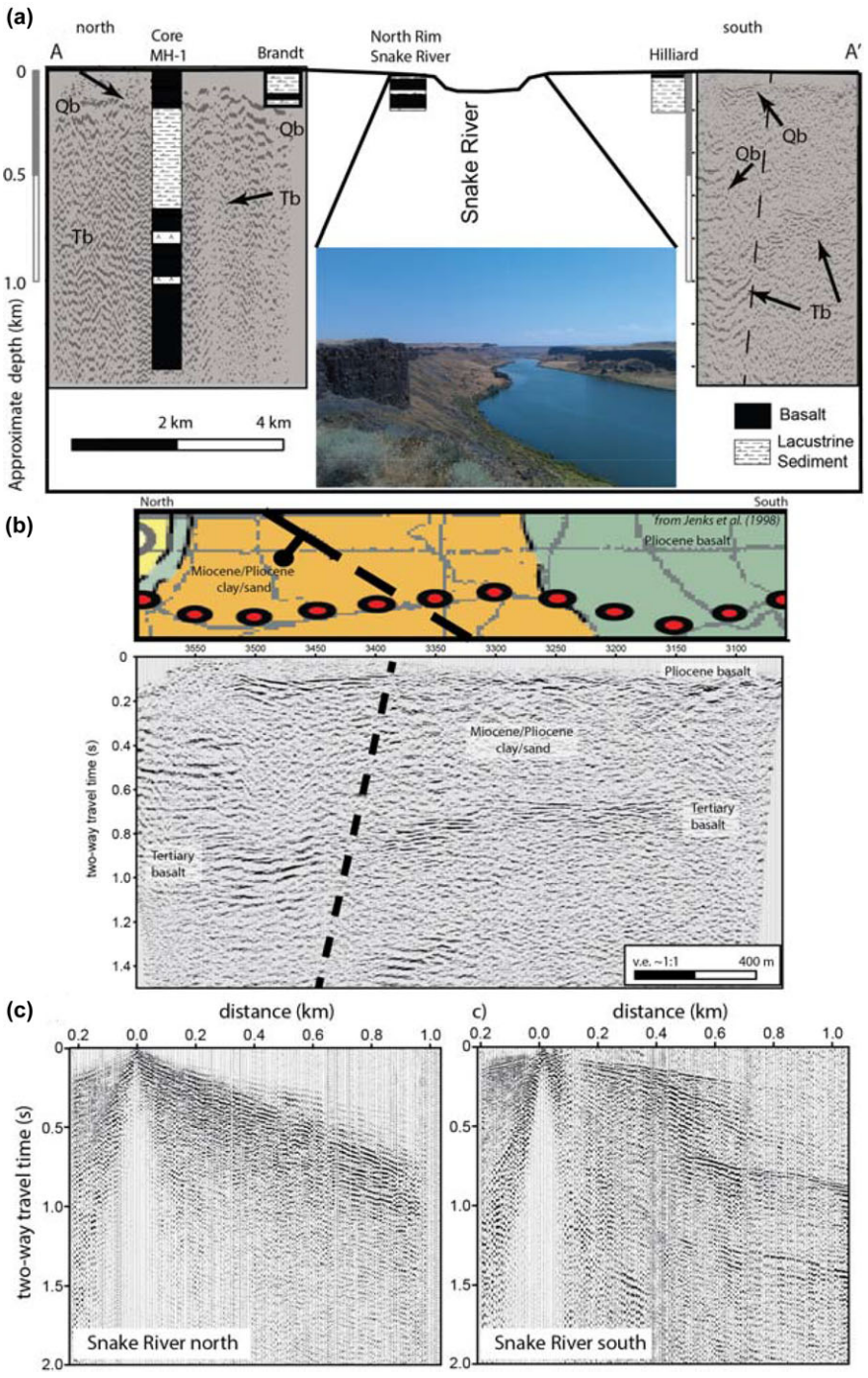

Figure 12 (a) Seismic reflection depth stacks from the Mountain Home area. Two P-wave seismic profiles that characterize surface Quaternary basalts (Qb), near-shore lacustrine sediments related to paleo Lake Idaho and underlying Tertiary basalts (Tb). Borehole logs are derived from nearby water wells. (b) Travel-time stack and surficial geologic map from the southern portion of the seismic profile (right-hand side of panel a) highlighting sediment and basalt reflections and reflector offsets across a mapped fault. (c) Shot gather from the northern and southern profile segments. Note the prominent reflectors on the southern profile shot gather from buried basalt layers. These reflections stack at approximately 1500 m/s and are not clearly identified on the profile north of the river.

We believe seismic imaging in volcanic terranes can be used to accurately map flow boundaries related to past eruptions, and if these flow boundaries are laterally continuous and are conduits to high-temperature fluid flow, seismic methods can be used to image targets related to geothermal exploration. That said, not all flow boundaries or sediment interbeds were imaged at all or with high confidence. This range of imaging capabilities highlights a significant problem with imaging in such complex environments. High-frequency signals are quickly attenuated at depth, suggesting that low-frequency signals are needed to image target depths of more than 1 km. Sediment interbed zones can also rapidly change thickness or material properties due to depositional or erosional conditions. Thus, reflection strength and static effects may simply vary along profiles to reflect subsurface conditions.

Wide-angle reflections that contain higher amplitude returns are beneficial to obtain quality reflection signals (e.g., Emsley, Boswell, and Davis 1998). Thus, our focus on reflected signals from offsets that approach imaging depths help produce interpretable results in the upper kilometre from all sites. However, without the use of geophone groups, reflections within the surface-wave window limited our reflection fold by muting the surface-wave window. A tie between borehole seismic measurements and subsurface physical property measurements may provide the necessary link between reflectivity and key target zones for geothermal exploration, particularly where mode conversions may appear. Additionally, a data acquisition strategy of large fold and possibly inline or 3D receiver groups may help attenuate both coherent and random noise, and improve data quality (e.g., Regone 1997), if only to be selective for the offsets that are included in the stack. Longer vibroseis sweeps that input a greater amount of high-frequency signals may also improve imaging results to resolve thin beds at great depths. As with other trends in reflection seismology, however, having lower frequencies would both improve penetration and resolution. Unfortunately, our source is not able to provide signal at frequencies below about 12 Hz. Processing steps that include a velocity model from borehole measurements, a layer stripping approach to build an accurate velocity model away from the borehole to address large static problems, and pre-stack migration methods may provide an improved seismic image in complex volcanic terranes.

CONCLUSIONS

Our seismic results suggest that a small vibroseis source is capable of imaging to geothermal target depths at a range of volcanic depositional environments. Surface and borehole seismic data show seismic imaging in the Snake River Plain sequence of volcanic rocks can identify some key stratigraphic horizons but requires a focus on detailed processing and acquisition design. Vertical seismic profiling results show increasing seismic velocities with depth within the volcanic rock sequence and suggest that low seismic attenuation at relatively low frequencies and large velocity contrasts are present. Surface seismic images show these large velocity contrasts are imaged, but data quality diminishes with increasing depth and confidence also decreases away from borehole locations. High fold to obtain wide-angle coverage is necessary, and high-frequency attenuation suggests that a focus on lower frequency acquisition will provide improved results. The potential for large static effects need to be addressed in processing, and with an accurate velocity model tied to borehole information, improved seismic imaging may be achieved with pre-stack migration methods.

ACKNOWLEDGEMENTS

Discussions with the Project Hotspot science team, and participants in the Project Hotspot planning workshops significantly added to our understanding and interpretations. We would like to thank the landowners who allowed us to drill on their property and provided their patient support throughout this process. This work was sponsored by DOE award DE-EE0002848, and by the International Continental Drilling Program (GFZ-Potsdam, Germany). ProMAX seismic processing software was provided by Landmark Graphics Corporation Strategic University Alliance Grant Agreement No. 2013-UGP-009000. Vista Processing software was employed directly in the field during data acquisition and this was provided to DRS by the former GEDCO, Calgary. The ICDP Operational Support Group led by Jochem Kück together with R. Kofman and L. Duerksen deserves particular recognition assisting in the extensive field program.

REFERENCES

Arney B.H. 1982. Evidence of former higher temperatures from alteration minerals, Bostic 1-A well, Mountain Home, Idaho. *Geothermal Resources Council Transactions* **6**, 3–6.

Burton A. and Lines L. 1997. VSP detection of interbed multiples using inside-outside corridor stacking. *Geophysics* **62**, 1628–1635.

Christensen N.I. 1982. Seismic velocities. In: *Handbook of Physical Properties of Rocks* Vol. **2**, pp. 1–228.

Christensen N.I., Fountain D.M., Carlson R.L. and Salisbury M.H. 1974. Velocities and elastic moduli of volcanic and sedimentary rocks recovered on DSDP Leg 25. In: *Initial Reports of the Deep*

Sea Drilling Project, *Vol.* **25** (eds E.S.W. Simpson et al.), pp. 357. U.S. Government Printing Office, Washington, USA.

Cox M. 1999. *Static Corrections for Seismic Reflection Surveys*. Society Exploration Geophysicists.

Emsley D., Boswell P. and Davis P. 1998. Sub-basalt imaging using long offset reflection seismic data. 60th EAGE Conference & Exhibition.

Hannsen P., Ziolkowski A. and Li X. 2003. A quantitative study on the use of converted waves for sub-basalt imaging, *Geophysical Prospecting*, 183–193.

Hubbell J.M., Bishop C.W., Johnson G.S. and Lucas J.G. 1997. Numerical ground-water flow modeling of the Snake River Plain aquifer using the superposition technique. *Ground Water* **35**(1), 59–66.

Jenks M.D., Bonnichsen B. and Godchaux M.M. 1998. *Geologic map of the Grandview-Bruneau area, Owyhee County, Idaho*, pp. 19. Idaho Geological Survey, University of Idaho.

Lindholm G.F. 1996. Summary of the Snake River regional aquifer-system analysis in Idaho and eastern Oregon. In: *U.S. Geological Survey Professional Paper 1408-A*, pp. 59.

Martini F. and Bean C.J. 2002. Interface scattering versus body scattering in subbasalt imaging and application of prestack wave equation datuming. *Geophysics* **67**(5), 1593–1601.

Nielson D.L., Delahunty C. and Shervais J.W. 2012. Geothermal systems in the Snake River Plain, Idaho, characterized by the hotspot project. *Geothermal Resources Council Transactions* **36**, 727–730.

Planke S., Alvestad E. and Eldholm O. 1999. Seismic characteristics of basaltic extrusive and intrusive rocks. *The Leading Edge* **18**(3), 342–348.

Pujol J., Fuller B. and Smithson S. 1989. Interpretation of a vertical seismic profile conducted in the Columbia Plateau basalts. *Geophysics* **54**(10), 1258–1266.

Pujol J. and Smithson S.B. 1991. Seismic wave attenuation in volcanic rocks from VSP experiments, *Geophysics* **56**(9), 1441–1455.

Regone C.J. 1997. Measurement and identification of 3-d coherent noise generated from irregular surface carbonates. In: *Carbonate Seismology*, pp. 281–305. Society of Exploration Geophysicists.

Schijns H., Heinonen S., Schmitt D.R., Kukkonen I.T. and Heikkinen P. 2009. Seismic refraction traveltime inversion for static corrections in a glaciated shield rock environment: A case study. *Geophysical Prospecting* **57**(9), 997–1008.

Schmitt D.R., Liberty L.M., Kessler J.E., Kück J., Kofman R., Bishop R. *et al*. 2012. The ICDP Snake River Geothermal Drilling Project: Preliminary overview of borehole geophysics. *Geothermal Resources Council Transactions*, 1017–1022.

Shervais J.W. and Hanan B.B. 2008. Lithospheric topography, tilted plumes, and the track of the Snake River–Yellowstone hot spot. *Tectonics* **27**, TC5004.

Shervais J.W., Evans J.P., Christiansen E.J., Schmitt D.R., Liberty L.M., Kessler J.E. *et al*. 2011. Hotspot: The Snake River Geothermal Drilling Project—An Overview. *Geothermal Resource Council Transactions*, **14**.

Shervais J.W., Nielson D.L., Evans J.P., Lachmar T., Christiansen E.H., Morgan L. *et al*. 2012. Hotspot: The Snake River Geothermal Drilling Project—Initial report. *Geothermal Resources Council Transactions* **36**, 767–772.

Stewart R.R., Gaiser J.E., Brown R.J. and Lawton D.C. 2003. Converted-wave seismic exploration: Applications. *Geophysics* **68**(1), 40–57.

Street L.V. and DeTar R.E. 1987. *Geothermal Resource Analysis in Twin Falls County, Idaho*. Idaho Department of Water Resources.

Twining B.V. and Bartholomay R.C. 2011. Geophysical logs and water-quality data collected for boreholes Kimama-1A and -1B, and a Kimama water supply well near Kimama, southern Idaho. *U.S. Geological Survey Data Series* **622**, 18.

Welhan J.A., Clemo T.M. and Gégo E.L. 2002. Stochastic simulation of aquifer heterogeneity in a layered basalt aquifer system, eastern Snake River Plain, Idaho. In: *Geology, Hydrogeology, and Environmental Remediation: Idaho National Engineering and Environmental Laboratory, Eastern Snake River Plain, Idaho, Geological Society of America Special Paper 353* (eds P.K. Link and L.L. Mink), pp. 225–247.

Widess M.B. 1973. How thin is a thin bed? *Geophysics* **38**(6), 1176–1180.

Wood S.H. 1994. Seismic expression and geological significance of a lacustrine delta in Neogene deposits of the western Snake River plain, Idaho. *AAPG Bulletin* **78** 1, 102–121.

Ziolkowski A., Hanssen P., Gatliff R., Jakubowicz H., Dobson A., Hampson G. *et al*. 2003. Use of low frequencies for sub-basalt imaging. *Geophysical Prospecting* **51**(3), 169–182.